Available online at www.sciencedirect.com
SCIENCE DIRECT®
ELSEVIER
International Journal of Mass Spectrometry 242 (2005) 43–48
International Journal of Mass Spectrometry
www.elsevier.com/locate/ijms

Intense femtosecond laser field-induced Coulomb fragmentation of C_2H_4

Ri Ma, Xia Li, Haizhen Ren, Hong Yang, Hongbing Jiang, Qihuang Gong*

State Key Laboratory for Mesoscopic Physics, Department of Physics, Peking University, Beijing 100871, People's Republic of China

Received 6 November 2004; accepted 19 November 2004
Available online 22 December 2004

Abstract

The fragments from Coulomb explosion of C_2H_4 irradiated by 130fs laser pulses at 810 nm wavelength and intensity around 10^{15} W/cm^2 are studied by using a time-of-flight mass spectrometer. The angular distributions of atomic ions exhibit anisotropy with the maximum along the laser polarization axis and the minimum perpendicular to it. The similar full width values at half maximum of angular distributions for C^{m+} ($m = 1$–3) ions imply a geometric alignment. On the other side, the singly and doubly charged molecular ions exhibit a markedly isotopic distribution. The dependence of the doubly charged parent ion $(C_2H_4)^{2+}$ on laser intensity indicates a nonsequential ionization mechanism.

JEL classification: 33.80.Wz; 42.65.Re; 33.15.Ta; 42.50.Hz

Keywords: Fragmentation; Ionization; Intense femtosecond laser; Coulomb explosion

---

1. Introduction

The interaction of hydrocarbons with intense femtosecond laser pulse has attracted much interest [1–4]. Various simple organic molecules, CH_4, C_2H_2, C_2H_4, C_3H_4 and C_3H_8 [1–5] have been studied. Under the intense laser field, the molecules can be ionized through multiphoton ionization process (MPI) or field ionization (FI) mechanism. In 1964, a value of Keldysh parameter [6] $\gamma = \omega(2m_e I_p)^{1/2}/eE$ was employed to characterize the ionization process, where I_p is the ionization energy, E is the electric field strength, ω is the angular frequency of the laser field, e and m_e are the electronic charge and mass, respectively. $\gamma \ll 1$ indicates FI and on the contrary, $\gamma \ll 1$ implies MPI.

For molecules suffered the MPI, the processes promote the electron to the continuum, involving the coherent absorption of a number of photons. When the laser field is strong enough (e.g., above 10^{14} W/cm^2), FI mechanism will become dominant. More than one electron can be stripped away from molecule related to tunneling process. Highly charged and unstably molecular ions can be generated due to the removal of several electrons from the molecule and the Coulomb explosion of parent ions leads to the generation of multiple charged atomic ions [7,8]. Usually, the kinetic energies of the fragment ions are substantially lower than that expected for prompt ionization or dissociation at equilibrium bond length R_e. Consequently, it is deduced that Coulomb explosion occurs at a critical distance R_c. For some small molecules, R_c is even about twice as large as R_e. Various models have been developed to interpret this reduction in Coulomb energy, for example, two-step model [9] and Tomas–Fermi–Dirac(TFD) model [10]. The critical distance R_c is supported to relax from the equilibrium R_e in all these models and where it stabilizes and subsequently ionizes with little or no change in inter-ion separation for the different ionization stages.

The fragment ions born in field ionization Coulomb explosion (FICE) usually exhibit anisotropic angular distributions as reported in our previous investigations on CO, CO_2, CS_2 [7,8,11]. The anisotropic angular distribution is attributed to the reorientation of the molecular axis and/or the dependence of the ionization rate on the angle between the laser field vector and the molecular dominant axis which indicates two

---

* Corresponding author. Tel.: +86 106 276 5884; fax: +86 106 275 6567.
E-mail address: qhgong@pku.edu.cn (Q. Gong).

1387-3806/$ – see front matter © 2004 Elsevier B.V. All rights reserved.
doi:10.1016/j.ijms.2004.11.013

effects: dynamic alignment and geometric alignment [12]. In the dynamic alignment mechanism, the intense laser fields distort the internal structure of molecules, and then induce a polarization within the molecules, which in turn interacts with the pulses. In the geometric mechanism, the pronounced anisotropy is attributed to the maximal ionization probability when the molecules axis is parallel to the laser electric field. In order to discriminate the two alignment mechanisms, a universal method using linearly and circularly polarized laser field has been proposed [13].

Nonsequential (NS) double and multiple ionization of molecules as another important phenomenon, which is related to multielectron effects in high intensity ultrashort-pulse laser, has been established as a challenging problem. NS ionization normally involves an enhancement on the double or multiple ionization yields instead of a sequential resonance process [14]. From the measurement of the cation and dication yields as a function of the laser intensity, the two-electron departing processes can be judged as NS ionization process or sequential ionization process. About NS ionization, a 'shake off' process [14] proposed by Fittinghoff et al. and electron–electron inelastic rescattering [15] proposed by Corkum have been used to explain the mechanism which may be influenced by the electronic states. In the case of N_2 and O_2, the experimental observations indicated that the detailed electronic structure plays a key role in NS double ionization yields [16].

In previous work, Talebpour et al. gave a report of radiationless transitions to various dissociation channels of ethylene molecular ion. The results showed fragmentation of the molecule occurs as a result of MPI of inner-valence electrons [1]. In this paper, the FICE of C_2H_4 is investigated by using a time-of-flight mass spectrometer (TOF-MS) in an intense laser field covering the intensity range of 0.5×10^{15} W/cm^2 to 9.3×10^{15} W/cm^2. Based on the results of the anisotropic angular distributions of C^{m+} ($m = 1$–3) ions from Coulomb explosion process, we get the conclusion that geometric alignment is responsible for the fragment anisotropy in the fs-laser-induced Coulomb explosion of C_2H_4. Especially, the production and enhancement of double charged parent ion $(C_2H_4)^{2+}$ shows the same result as that of molecules [16,17] N_2 and O_2, which indicate electrons ejection can be a NS process at some intensity range. And NS ionization mechanism may be due to the complicated molecular structure which is strongly coupled with a fs-pulse laser field.

2. Experimental system

The experimental setup has been described in detail in our previous report [18]. A Ti:sapphire CPA laser system (TSA-10, Spectra-Physics Inc., USA), which delivers 810 nm, 130 fs pulses at a repetition rate of 10 Hz, was employed as the light source. The laser beam was focused by a lens with focal length 15 cm into the chamber of the TOF-MS.

The TOF-MS used here was a Wiley-McLaren-type time-of-flight mass spectrometer with a drift tube of 35 cm in length [19]. The vacuum chamber can be pumped to an ultimate pressure of 10^{-5} Pa. A C_2H_4 gas sample was introduced into the chamber via a pulsed valve (Park Inc., USA) with a 0.2 mm orifice. When the gas sample was admitted, the chamber pressure was maintained to be at several 10^{-4} Pa to avoid the space-charge effect [20] and pressure broadening of the ion peaks. A microchannel plate assembly was used to detect the ions. The signals were recorded using ultrahigh speed data acquisition card (DP110, Acqiris Digitizers, Switzerland) with a maximal real-time sampling rate of 1 GHz. The signals were typically averaged over 256 laser pulses. The pulsed valve, the data acquisition card and the femtosecond laser pulses were timing scheduled by a DG535 digital delay and pulse generator (Stanford Research Systems, USA).

In order to measure the angular distribution, a half-waveplate was inserted into the path of the laser beam to rotate the electric field vector with an angle interval of 4°. In the measurement, the polarization angle is defined as the angle between the axis of the TOF-MS and the polarization vector of the laser field.

3. Results and discussion

3.1. Mass spectra of C_2H_4

The typical time-of-flight mass spectra of ethylene molecule are shown in Fig. 1, irradiated by 810 nm, 130 fs laser pulse at intensity 7.6×10^{15} W/cm^2. The linearly polarized laser fields are used in (a) while the circularly polarized laser fields are used in (b). Abundant fragment ions H^+ and C^{m+} ($m = 1$–3) are observed. The marked double-peak structure of C^{m+} ($m = 1$–3) ions indicates a FICE process in (a). This is in agreement with the calculated value of Keldysh parameter $\gamma = 0.11$ ($\gamma \ll 1$ means FI mechanism). The observed H_2O molecular ions are from residual water in the vacuum chamber. From Fig. 1, the parent precursor ${C_2H_4}^+$ produced

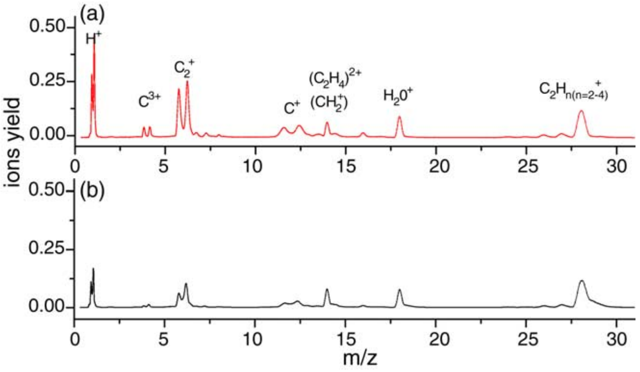

Fig. 1. TOF mass spectra of C_2H_4 induced by 810 nm, 130 fs laser pulses at intensity 7.6×10^{15} W/cm^2. The horizontally polarized laser fields are used in (a) while the circularly polarized light is used in (b).

by nonresonant ionization is much larger than that of $C_2H_3^+$ and $C_2H_2^+$ ions. The only appearance of CH_2^+ and $(C_2H_4)^{2+}$ near the value of *m*/*z* with 14 in the mass spectrum of Fig. 1, indicates no channels originated from $C_2H_3^{2+} \rightarrow CH_2^+ + CH^+$ and $C_2H_2^{2+} \rightarrow CH^+ + CH^+$. Because if there existed the above two channels, the fragment ion CH^+ should be observed. Due to the π electronic structure of ethylene, C_2H_4 just exhibited the direct explosion and ionization with little kinetic energy release. So the three peaks where the value of *m*/*z* is 14, afforded sufficient evidence. The middle $(C_2H_4)^{2+}$ ions of the three peaks structure are just coming from the ionized parent molecules. Few $C_2H_3^+$ and $C_2H_2^+$ ions also supported the result with no CH^+ ions in existence. Considerable suppression of ionization shown in the case of circular polarization in (b) agrees well with the predictions of FI mechanism. Because for circularly polarized light with the rotating E-field vector, the electrons have no enough time to traverse the tunnel barrier before the E vector changes in the FI model.

We have also measured the mass spectrum of ethylene at different laser intensities. Fig. 2 shows the results at the range of 0.5×10^{15} W/cm^2 to 9.3×10^{15} W/cm^2. All the ionic signals increase with increment on laser intensity. When the intensity is lower than 1.7×10^{15} W/cm^2, only molecular ions are observed, and the fragment C^{3+} ions could only be observed at the intensity above 2.7×10^{15} W/cm^2. The sequent appearance of C^+, C^{2+} to C^{3+} is consistent with the fact that the steady increase in the ionization energy for C^+, C^{2+} to C^{3+}, which are 11.260 eV, 24.383 eV and 47.887 eV, respectively.

3.2. Kinetic energy release (KER) and angular distributions

The KER of atomic ions from the Coulomb explosion can be determined from the peak splitting in the mass spectrum according to [21]:

$$E_{\text{kinetic energy}} = \frac{(U_1 - U_2)^2}{8md^2} q^2 \Delta t^2 \qquad (1)$$

where *d* is the distance between the repeller plate and the first acceleration plate, *q* is the charge of the ion and Δt is the arrival time difference between forward and backward ejected ions, *m* is the mass of the fragment ion. For the light atoms such as H and C, the value of $C_m{}^{-1}$ in $R_c = C_m{}^{-1} R_e$ adopted 0.45, which should be valid for ethylene [4]. So the theoretical values are calculated by analyzing the instantaneous Coulomb repulsion process. The bond length of C–H and C–C are 1.071 Å and 1.353 Å, respectively, and the angle of H–C–H is 120°. In Table 1, we listed the measured kinetic energies of C^{m+} ($m = 1$–3) at laser intensity of 7.6×10^{15} W/cm^2. By comparing the measured kinetic energies of atomic ions and the calculated ones, we can identify the Coulomb explosion channels: C^+ mainly from (1, 1), (1, 2) channels and C^{2+} mainly from (2, 1), (2, 2) channels. Moreover, the calculation for (*p*, *q*) ($p = q = 1$, 2) channel approaches closely to the experimental values. It may be noted that the charge-symmetric fragmentations are much favored in our Coulomb explosive experiment.

The angular distributions of atomic and molecular ions are shown in Fig. 3. The isotropic distributions of singly and doubly charged parent ions $C_2H_4^+$ and $(C_2H_4)^{2+}$ differ remarkably from the anisotropic distributions of C^{m+} ($m = 1$–3) fragment ions. And the signal intensity of C^{2+} ions is stronger than that of singly and triply charged carbon ions. The principal structure of C–C bond is very similar with that of some diatomic molecules, such CO and N_2 [7,22]. When the polarization vector is parallel to the TOF-MS axis, for the very large electronegative difference of H and C atom, the couple of C–C along the axis is more valid than that of other directions just like C–H bonds. The FWHM values of C^{m+} ($m = 1$–3) ions' angular distributions calculated by a Gaussian fitting (seen in Table 1), support the observation [23] of almost same angular distributions for different charged atomic ions, which would imply a geometric alignment. While as for the

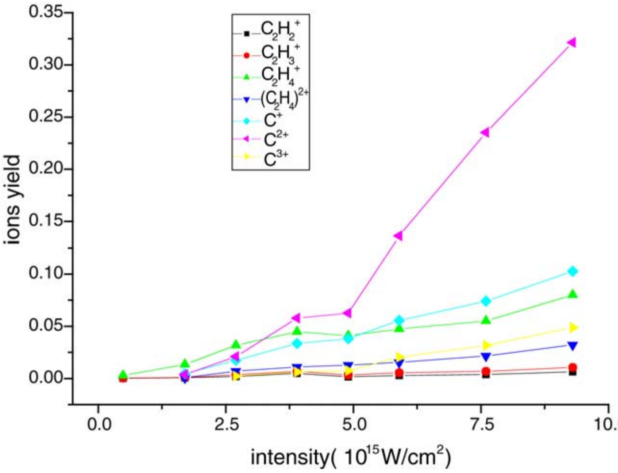

Fig. 2. Variation of atomic and parent ion yields from ethylene molecules with laser intensity.

Table 1
The KER at an intensity of 7.6×10^{15} W/cm^2 and the theoretical Coulomb repulsive energy at a critical internuclear distance $R_c = C_m{}^{-1} R_e$

Ions	FWHM (°)	E_{exp} (eV)	Channels (*p*, *q*)	*E* (eV) (theoretical)
C^+	41.6 ± 2.5	3.44	(1, 1)	2.35
			(1, 2)	4.75
			(1, 3)	7.13
C^{2+}	39.7 ± 1.2	8.24	(2, 1)	4.71
			(2, 2)	9.49
			(2, 3)	14.3
C^{3+}	43.7 ± 1.8	13.9	(3, 1)	7.09
			(3, 2)	14.2
			(3, 3)	21.4

The notation (*p*, *q*) ($p = 1$–3, $q = 1$–3) stands for the Coulomb explosion channel (C^{p+}, C^{q+}).

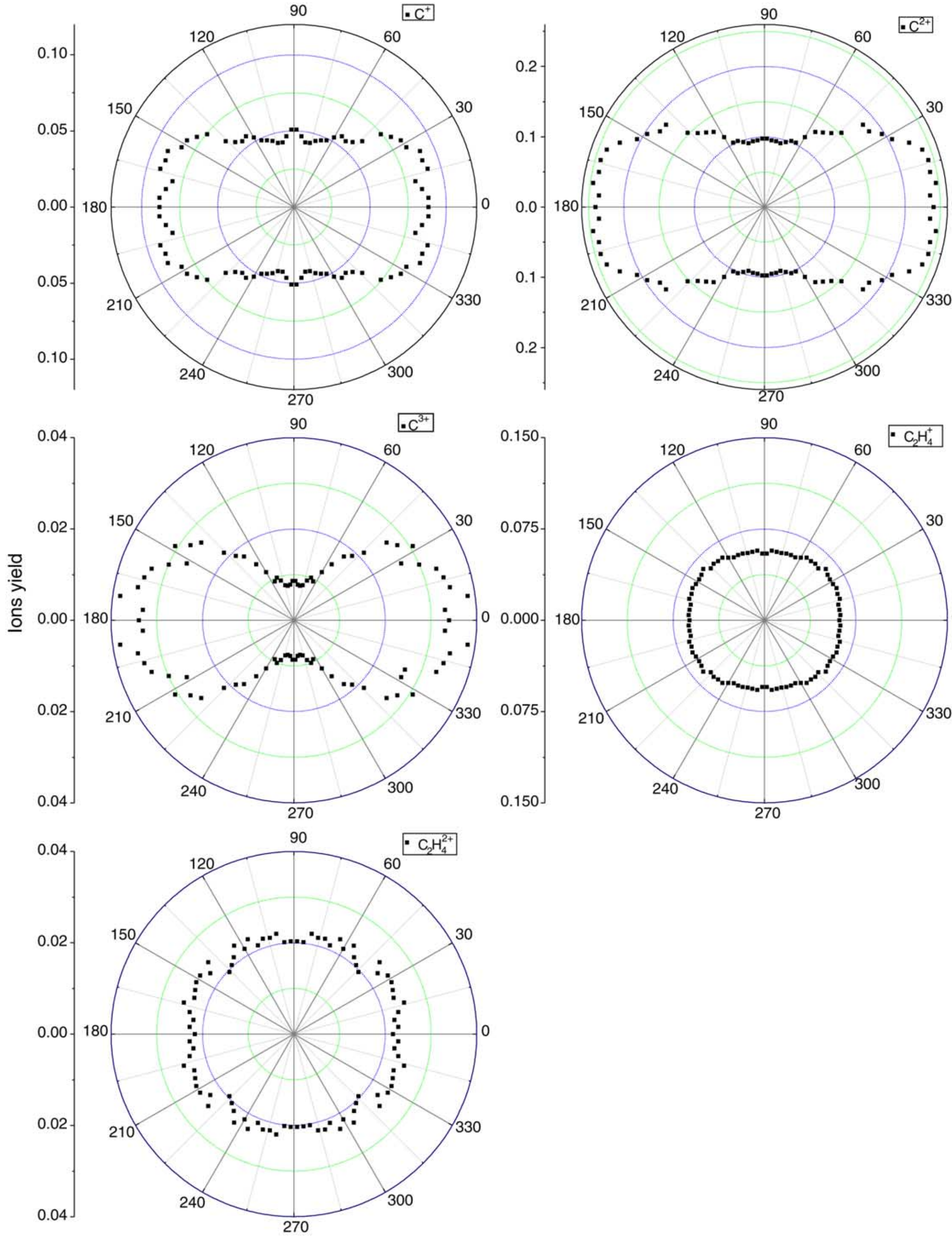

Fig. 3. Anisotropic distributions of the observed carbon ions from the FICE process and isotropic distributions of molecular ions at the laser pulse intensity of 7.6×10^{15} W/cm^2.

dynamic alignment, the higher charged states, the narrower angular distributions.

3.3. Ellipticity effects and nonsequential ionization

Fig. 4 shows the trend of ion signals as a function of ellipticity of laser polarization $\varepsilon = E_x/E_y$. The y direction is along the TOF-MS axis. $\varepsilon = 0$ corresponds to the linear polarization and $\varepsilon = 1$ represents the circularly polarized laser field. It is noted that the carbon atomic ion yields decrease monotonically when ε varied from 0 to 1. This may be attributed to that the electric field effective component coupling with the C–C bond decreases in changing from linear polarization to circular polarization at the same laser intensity. For the reason, we calculated the ratio of C^{m+} ($m = 2, 3$) with circularly polarized at light intensity of 7.6×10^{15} W/cm^2 to with

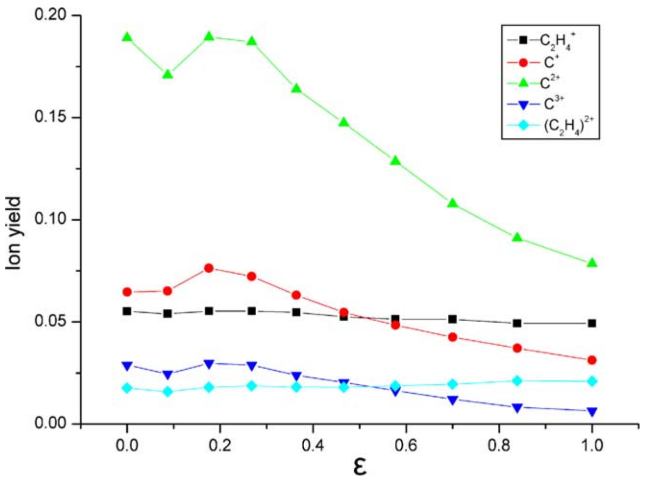

Fig. 4. Dependence of atomic and parent ion yields on ellipticity ε at the laser intensity of 7.6×10^{15} W/cm^2. $\varepsilon = 0$ denotes linearly polarized light, with the field vector parallel to the TOF-MS axis. $\varepsilon = 1$ denotes circularly polarized light.

p-polarization light at intensity 3.8×10^{15} W/cm^2, which are 1.36 and 1.08, respectively. The laser intensity is doubled in the circularly polarization in order to ensure that the field amplitude is equal in the two polarized states. The results are also in disagreement with the prediction of dynamic alignment, which indicates the ions yields should be highly suppressed in the circularly polarized field compared to the linearly polarized light in the same field amplitude. Therefore, geometric alignment is responsible for the anisotropic angular distributions, which is similar to the results of our earlier work on C_2H_6 molecule [24].

The observation of isotropic distributions of singly and doubly molecular parent ions: $C_2H_4^+$ and $(C_2H_4)^{2+}$ in Fig. 3 is consistent with the results of our early experiments on diatomic and triatomic parent precursor [8,22]. The dependence of $(C_2H_4)^{2+}/C_2H_4^+$ on laser intensity is shown in Fig. 5. It shows the ratio has a strong dependence on laser intensity as it is below 7.6×10^{15}W/cm^2. And on the contrary, a weak dependence on intensity is observed above 7.6×10^{15}W/cm^2. This reveals that the precursor of $(C_2H_4)^{2+}$ is not $C_2H_4^+$, and the ionization involves the nonsequential(NS) process [16,25,26]. If $(C_2H_4)^{2+}$ is produced in a sequential process, $C_2H_4^+$ will be the intermediate species and the ratio of $(C_2H_4)^{2+}/C_2H_4^+$ will reflect the ionization rate from $C_2H_4^+$ to $(C_2H_4)^{2+}$ which will afford a strong intensity dependence.

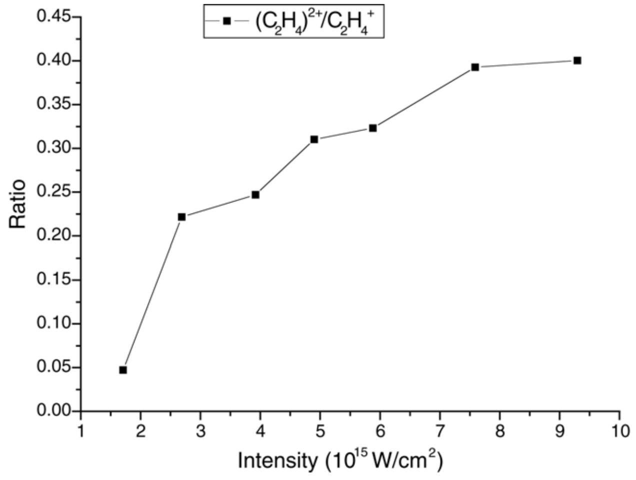

Fig. 5. Ratio curve of $(C_2H_4)^{2+}/C_2H_4^+$ at different laser intensity with linearly polarized light.

4. Conclusions

Coulomb exploding fragments and molecular ions of ethylene molecule are measured and discussed at $\sim 10^{15}$ W/cm^2 intensity range. Instantaneous spatial alignment is occurring during the FICE process. The fact that the similar widths of anisotropic distributions of carbon atomic ions implies a geometric alignment mechanism, which is further approved by the measurements on the ratios of C^{m+} ($m = 2, 3$) with circularly polarization to with p-polarization light at equal intensity. Moreover, NS ionization is observed to be dominant at laser intensity lower than 7.6×10^{15}W/cm^2.

Acknowledgements

This work supported by the National Key Basic Research Special Foundation (NKBRSF) under grant no. TG1999075207, the National Natural Science Foundation of China under grant nos. 10104003, 90206003, 10328407 and 90101027.

References

[1] A. Talebpour, A.D. Bandrauk, J. Yang, S.L. Chin, Chem. Phys. Lett. 313 (1999) 789.
[2] C. Cornaggia, Phys. Rev. A 52 (1995) 4328.
[3] C. Cornaggia, M. Schmidt, D. Normand, Phys. Rev. A 51 (1995) 1431.
[4] C. Cornaggia, D. Normand, J. Morellec, J. Phys. B: At. Mol. Opt. Phys. 25 (1992) 415.
[5] C.Y. Wu, H.Z. Ren, T.T. Liu, R. Ma, H. Yang, H.B. Jiang, Q.H. Gong, J. Phys. B: At. Mol. Opt. Phys. 35 (2002) 2575.
[6] L.V. Keldysh, Sov. Phys. JETP 20 (1965) 1307.
[7] H.Z. Ren, R. Ma, J.X. Chen, X. Li, H. Yang, Q.H. Gong, J. Phys. B: At. Mol. Opt. Phys. 36 (2003) 2179.
[8] J.X. Chen, H.Z. Ren, R. Ma, X. Li, H. Yang, Q.H. Gong, Int. J. Mass Spectrom. 228 (2003) 81.
[9] S. Chelkowski, A.D. Bandrauk, J. Phys. B: At. Mol. Opt. Phys. 28 (1995) 723.
[10] M. Brewczyk, L.J. Frasinski, J. Phys. B: At. Mol. Opt. Phys. 24 (1991) 307.
[11] C.Y. Wu, H.Z. Ren, T.T. Liu, R. Ma, H. Yang, H.B. Jiang, Q.H. Gong, Int. J. Mass. Spectrom. 12111 (2002) 1.
[12] J.H. Posthumus, J. Plumridge, M.K. Thomas, K. Colding, L.J. Frasinski, A.J. Langely, P.F. Taday, J. Phys. B: At. Mol. Opt. Phys. 31 (1998) 553.
[13] Ch. Ellert, P.B. Corkum, Phys. Rev. A 59 (1999) 3170.

[14] D.N. Fittingoff, P.R. Bolton, B. Chang, K.C. Kulander, Phys. Rev. Lett. 69 (1992) 2642.
[15] P.B. Corkum, Phys. Rev. Lett. 71 (1993) 1994.
[16] C.L. Guo, M. Li, J.P. Nibarger, G.N. Gibson, Phys. Rev. A 61 (2000) 033413.
[17] C.L. Guo, G.N. Gibson, Phys. Rev. A 63 (2001) 040701.
[18] C.Y. Wu, H.Z. Ren, T.T. Liu, R. Ma, H. Yang, H.B. Jiang, Q.H. Gong, Int. J. Mass Spectrom. 216 (2002) 249.
[19] W.C. Wiley, I.H. Mclaren, Rev. Sci. Instrum. 26 (1955) 1150.
[20] M.V. Ammosov, F.A. Il'kov, M.G. Malakhov, Ch. K. Mukhtarov, J. Opt. Soc. Am. B 6 (1989) 1961.
[21] S. Shimizu, J. Kou, S. Kawato, K. Shimizu, S. Sakabe, N. Nakashima, Chem. Phys. Lett. 317 (2000) 609.
[22] C.Y. Wu, H.Z. Ren, T.T. Liu, R. Ma, H. Yang, H.B. Jiang, Q.H. Gong, Appl. Phys. B 75 (2002) 91.
[23] P. Graham, K.W.D. Ledingham, R.P. Singhai, S.M. Hankin, T. McCanny, X. Fang, C. Kosmidis, P. Tzallas, P.F. Taday, A.J. Langley, J. Phys. B: At. Mol. Opt. Phys. 34 (2001) 4015.
[24] X. Li, H.Z. Ren, R. Ma, J.X. Chen, H. Yang, Q.H. Gong, Chin. Phys. 13 (2004) 1564.
[25] C.L. Guo, G.N. Gibson, Phys. Rev. A 63 (2001) 040701.
[26] C.L. Guo, M. Li, J.P. Nibarger, G.N. Gibson, Phys. Rev. A 58 (1998) 4271.